

CHANGE OF SEA SURFACE HEIGHT IN THE EAST ASIA SEAS FROM SATELLITE ALTIMETER DATA

Chung-Ru Ho^{*1}, Yu-Hsin Cheng², Nan-Jung Kuo³, and Shih-Jen Huang⁴

¹Professor, Department of Marine Environmental Informatics, National Taiwan Ocean University
2, Pei-Ning Rd., Keelung 20224, Taiwan; Tel: +886-2-24622192#6331
E-mail: b0211@mail.ntou.edu.tw

²Graduate Student, Department of Marine Environmental Informatics, National Taiwan Ocean University
2, Pei-Ning Rd., Keelung 20224, Taiwan; Tel: +886-2-24622192#6345
E-mail: 29981002@mail.ntou.edu.tw

³Professor, Department of Marine Environmental Informatics, National Taiwan Ocean University
2, Pei-Ning Rd., Keelung 20224, Taiwan; Tel: +886-2-24622192#6316
E-mail: c0021@mail.ntou.edu.tw

⁴Assistant Professor, Department of Marine Environmental Informatics, National Taiwan Ocean University
2, Pei-Ning Rd., Keelung 20224, Taiwan; Tel: +886-2-24622192#6319
E-mail: huangsj@mail.ntou.edu.tw

KEY WORDS: Altimeter, Sea surface height, East Asia Seas, Trend, ENSO

ABSTRACT: The change of sea surface height (SSH) in the East Asia Seas (10~40 °N, 110~130 °E) from 1993 to 2010 is investigated using satellite altimeter data. From the linear regression analysis, the SSH has an increasing rate of 5.3 mm/year in the study area. However the increasing rate of SSH is different in seasons. The highest and the lowest increasing rate are 5.5 mm/year and 4.2 mm/year in fall and in winter, respectively. We further divided the study region into four parts which are the Yellow Sea, the East China Sea, the Sea of Philippine basin, and the South China Sea, respectively. The results show that the highest increasing rate is 5.8 mm/year in the South China Sea and the variation of SSH is also related to the El Niño/Southern Oscillation (ENSO) index with a correlation coefficient of 0.75.

1. INTRODUCTION

Since global climate has been severely changing, and caused numerous disasters and casualties around the world, remote sensing has become more important in dealing with this situation. Sea level is one of the indicators of global change because the main contributions to the sea level rise include ocean thermal expansion and melting of land ices. According to the IPCC 4th Assessment Report published in 2007 (Bindoff et al., 2007), global mean sea level has been raised 1.8 mm/year (1.3-2.3 mm/year) since 1961 and the average rising rate is 3.1 mm/year during the 1993–2003 decade. Using tide-gauge data, Gornitz et al. (1982) found that the sea level trend is 1.2 mm/year in the world ocean from 1880-1980 and indicated that the sea level change has a high correlation with the trend of global surface air temperature. A large part of the sea level rise can be accounted for in terms of the thermal expansion of the upper layers of the ocean. A similar result was found by Douglas (1991) that the value of mean sea level rise from a global set of 21 stations is 1.8 mm/year from 1880-1980. Church and White (2006) analyzed sea level change using tide-gauge data from 1950 to 2000 and found a larger rate of rise after 1993. Using space gravimetry observations from GRACE, Cazenave et al. (2009) showed that recent years' sea level rise can be mostly explained by an increase of the mass of the oceans. However, the local effects of sediment unloading and loading on ocean bathymetry may be the same as that caused by mass change in ice and meltwater over glacial on the global scale (Raymo et al., 2011; Shennan, 2011). A recent report from newsroom of Jet Propulsion Laboratory/National Aeronautics and Space Administration (JPL/NASA) website, the global sea level drop of nearly 6 mm in 2010 is attributable to the switch El Niño to La Niña conditions in the Pacific. It means that the influences of sea level changes are not only by the thermal expansion and melting glaciers and ice caps, but also by the local effect.

In this study, we will use the sea surface height (SSH) data derived from satellite altimeters to investigate the local effect under the global change. The study area is focus on the East Asia Seas ranged from 10 °N to 40 °N in latitude and from 110 °E to 130 °E in longitude. To get more detail information, we further divided the study area into 4 sub-regions, that is, the Yellow Sea (YS) from 34 °N to 40 °N and from 120 °E to 127.5 °E, the East China Sea (ECS) from 25 °N to 34 °N and from 120 °E to 130 °E, the Sea of Philippine basin (PS) from 15 °N to 25 °N and from 120 °E to 130 °E, and the South China Sea (SCS) from 10 °N to 22.5 °N and from 110 °E to 120 °E as shown in Figure 1.

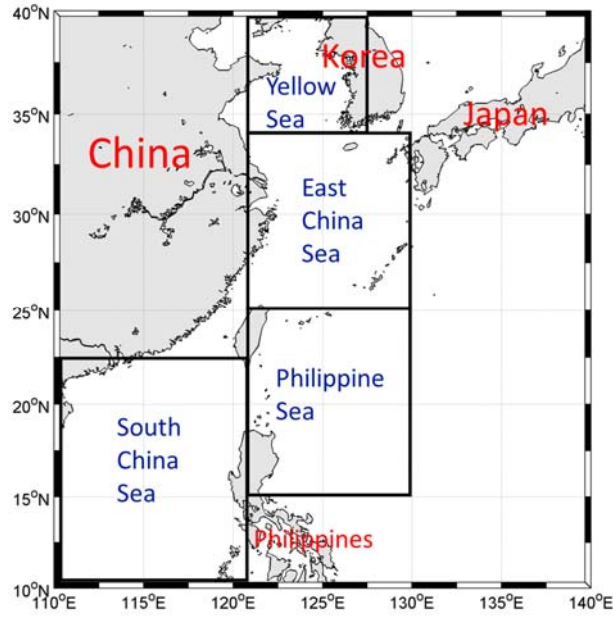


Figure 1. The study area.

2. DATA

2.1 Sea Surface Height Data

The SSH data used in this study is acquired from AVISO (Archiving, Validation and Interpretation of Satellite Oceanographic data program). The dataset is monthly mean and is derived from multi-satellite altimetry measurements including ERS-1/2 (Europe Remote Sensing), T/P (TOPEX/Poseidon), GFO (Geosat Follow-on), ENVISAT (Environmental Satellites), and Jason-1/2. Its spatial resolution is 0.25° by 0.25°. The accuracy of the dataset is about 4.3 cm (Tapley et al., 1996). To avoid the local fluctuation, we further averaged the 0.25° dataset into 1° dataset. The data period we used is from 1993 to 2010.

2.2 Southern Oscillation Index

The Southern Oscillation Index (SOI) is calculated from the monthly fluctuations in the air pressure difference between Tahiti and Darwin. Actually, there are many different methods of how to calculate the SOI. Here we used the Troup SOI which is the standardized anomaly of the mean sea level pressure (MSLP) difference between Tahiti and Darwin. It is calculated as follows:

$$SOI = 10 \times \frac{P_{diff} - P_{diffav}}{SD(P_{diff})} \quad (1)$$

where P_{diff} is the difference between average Tahiti MSLP for the month and average Darwin MSLP for the month, P_{diffav} is the long term average of P_{diff} for the month, and $SD(P_{diff})$ is long term standard deviation of P_{diff} for the month. The multiplication by 10 is a convention. A strongly and consistently positive SOI pattern is La Niña. Conversely, a strong and consistently negative SOI pattern is El Niño. In this study, the SOI data is obtained from the Australia Bureau of Meteorology at <http://www.bom.gov.au/climate/current/soihtm1.shtml>.

3. RESULTS

3.1 Sea Surface Height Variations

Figure 2 shows the SSH anomaly (SSHA) variation in the study area from 1993 to 2010. An increasing trend of 5.3 mm/year is obviously found. However, the increasing trend is different in the four sub-areas. The YS and the ECS regions have much lower increasing trends than those in the PS and SCS regions. As shown in Figure 3, the increasing trends of SSHAs are 3.7 mm/year in YS, 3.8 mm/year in ECS, 5.7 mm/year in PS and 5.8 mm/year in SCS, respectively. This indicates that the thermal expansion effect on the SSH is higher in the tropical ocean than that in the sub-tropical and temperate oceans.

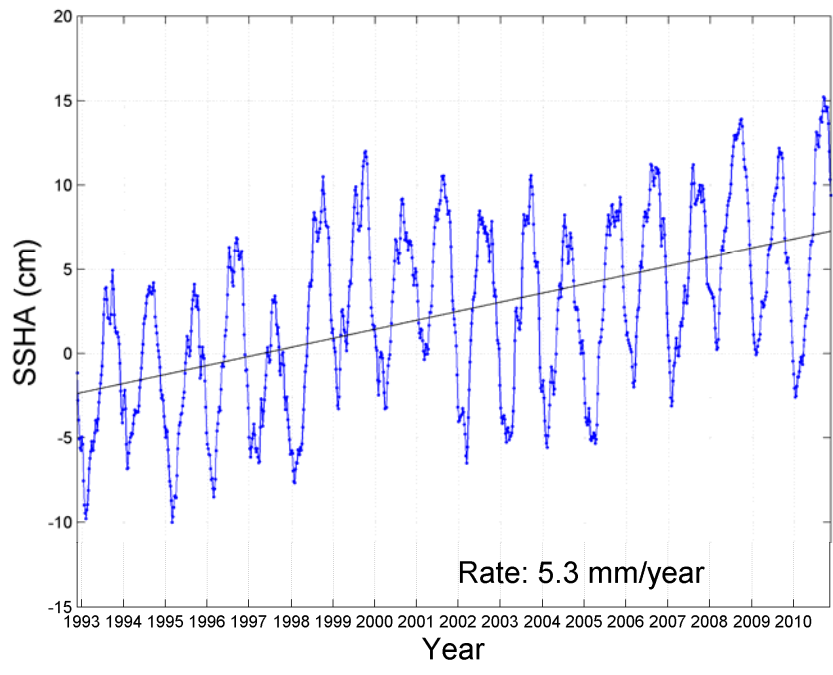


Figure 2. The SSH variation in the study area. The straight line is the trend of SSH.

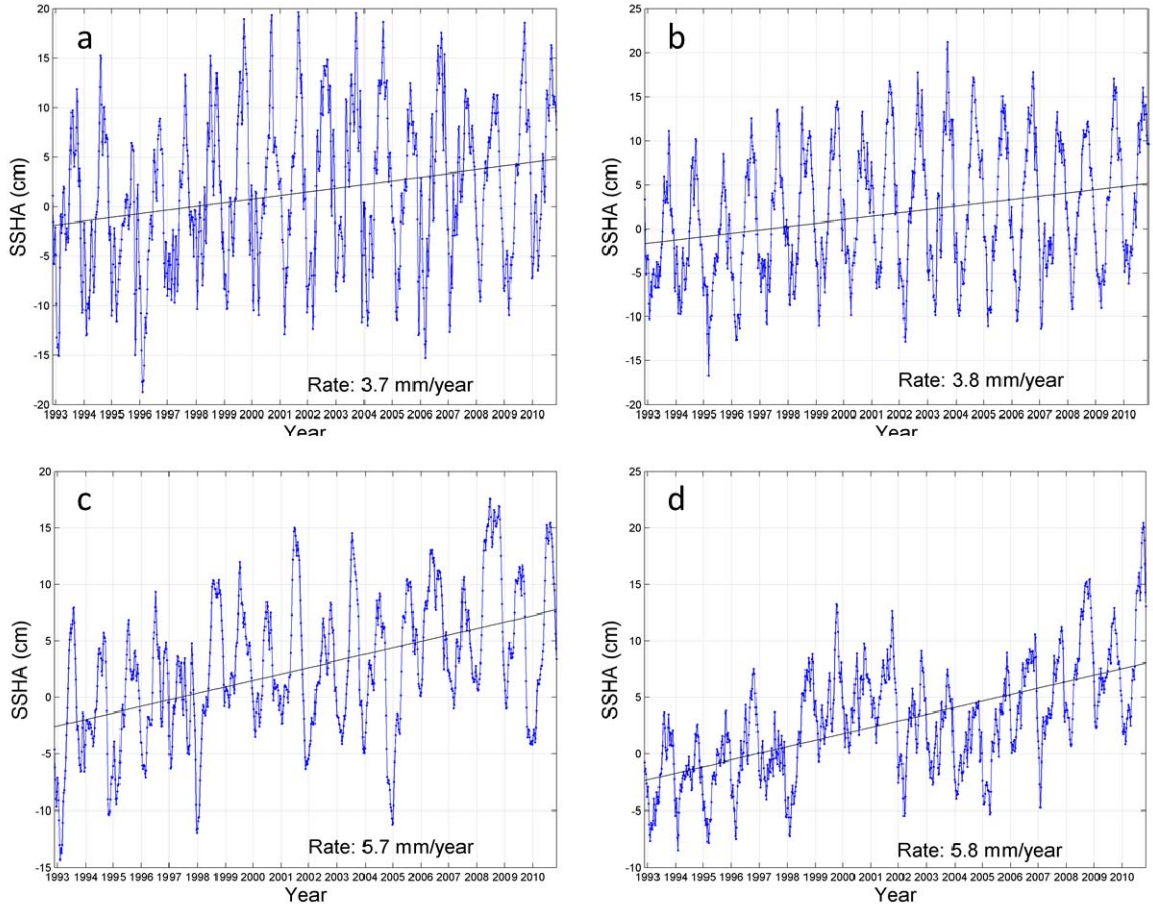


Figure 3. The SSH variation in the four sub-areas: (a) Yellow Sea; (b) East China Sea; (c) Philippine Sea; and (d) South China Sea. The straight line is the trend of SSH.

3.2 Seasonal Trends

As above-mentioned, the thermal expansion could be a key role in the effect of SSH. Therefore, the seasonal trends of SSHA could be also different. Figure 4 shows the seasonal trends of SSHA in the study area. Fall and winter have the highest and the lowest increasing trends of 5.5 mm/year and 4.2 mm/year. Spring and summer have the same increasing trend of 5.2 mm/year, almost the same as that in fall. This phenomenon implies the thermal effect is important to SSH change.

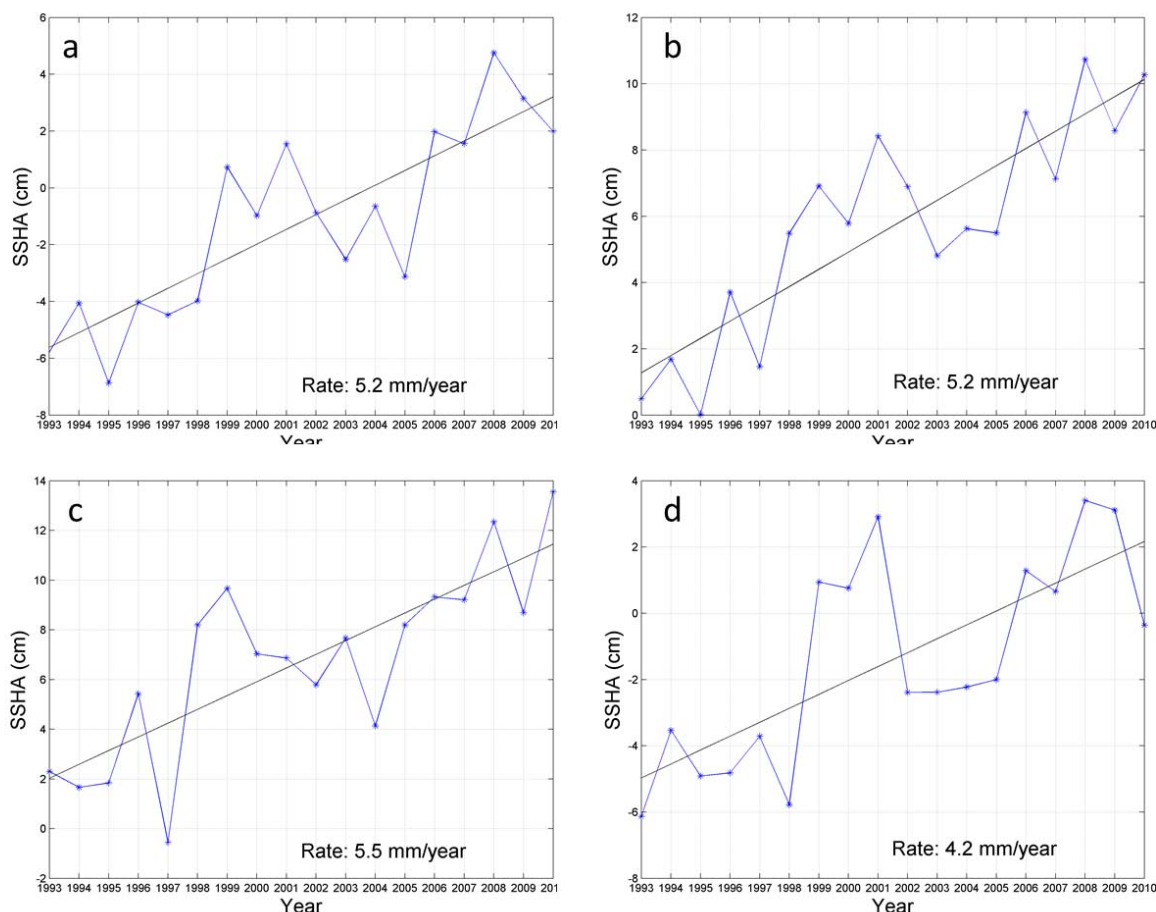


Figure 4. The SSHA trends in the whole study area in (a) spring; (b) summer; (c) fall; and (d) winter.

3.4 Influence of ENSO

To inspect the influence of El Niño/Southern Oscillation (ENSO) on the SSH variations, we compute the correlation coefficient (R) between yearly mean SSHA and SOI to remove the effect of short-term variations. For the entire study area, the R is 0.75. However the R increases from temperate oceans to tropical oceans, that is, from YS to SCS (Table 1). This implies that the SSH variation may be affected more obviously by the ENSO events if the area is closer to the tropical Pacific.

Table 1. The correlation coefficient between SSH and SOI

	East Asia Seas	Yellow Sea	East China Sea	Philippine Sea	South China Sea
Correlation Coefficient	0.75	0.33	0.46	0.71	0.77

4. SUMMARY

The trends of sea surface height in the East Asia Seas are investigated by using satellite altimeter data. The results are summarized as follows. 1) The SSH in the East Asia Sea has an increasing trend of 5.3 mm/year from 1993 to

2010. 2) The increasing trend is different in seasons. Due to the storage of heat from summer, fall has the largest increasing trend because of the thermal expansion effect. 3) The SCS has the largest increasing trend in the four different regions because the SCS is in the tropical ocean where the highest heat storage has. 4) The SSH variation is also affected by ENSO events, especially in the SCS because it is a part of the Western Pacific Warm Pool (Lin et al., 2011) where it is strongly related to the ENSO events.

ACKNOWLEDGMENTS

The authors appreciate AVSIO and the Australia Bureau of Meteorology for providing the SSH data and the SOI data, respectively. This work is partly supported by the National Science Council (NSC) of Taiwan through grant NSC 98-2611-M-019-017-MY3.

REFERENCES

- Bindoff, N.L., J. Willebrand, V. Artale, A. Cazenave, J. Gregory, S. Gulev, K. Hanawa, C. Le Quéré, S. Levitus, Y. Nojiri, C.K. Shum, L.D. Talley and A. Unnikrishnan, 2007. Observations: Oceanic Climate Change and Sea Level. In: *Climate Change 2007: The Physical Science Basis. Contribution of Working Group I to the Fourth Assessment Report of the Intergovernmental Panel on Climate Change*, edited by Solomon, S., D. Qin, M. Manning, Z. Chen, M. Marquis, K.B. Averyt, M. Tignor and H.L. Miller, Cambridge University Press, Cambridge, United Kingdom and New York, NY, USA.
- Cazenave, A., K. Dominh, S. Guinehut, E. Berthier, W. Llovel, G. Ramillien, M. Ablain and G. Larnicol, 2009. Sea level budget over 2003–2008: A reevaluation from GRACE space gravimetry, satellite altimetry and Argo. *Global and Planetary Change*, 63, pp. 83-88.
- Church, J. A., and N. J. White, 2006. A 20th century acceleration in global sea-level rise. *Geophysical Research Letters*, 33, L01602, doi:10.1029/2005GL024826.
- Douglas, B. C., 1991. Global sea level rise. *Journal of Geophysical Research*, 96(C4), pp. 6981-6992.
- Gornitz, V., B. Lebedeff and J. Hansen, 1982. Global sea level trend in the past century. *Science*, 215, pp. 1611-1614.
- Lin, C.-Y., C.-R. Ho, Q. Zheng, S.-J. Huang, and N.-J. Kuo, 2011. Variability of sea surface temperature and warm pool area in the South China Sea and its relationship to the western Pacific warm pool. *Journal of Oceanography*, (Accepted).
- Raymo, M. E., J. X. Mitrovica, M. J. O’Leary, R. M. DeConto, and P. J. Hearty, 2011. Departures from eustasy in Pliocene sea-level records. *Nature Geoscience*, 4, pp. 328-332.
- Shennan, I., 2011. Sea level from global to local. *Nature Geoscience*, 4, pp. 283-284.
- Tapley, B. D., M. M. Watkins, J. C. Rise, G. W. Davis, R. J. Eanes, S. R. Poole, H. J. Rim, B. E. Schutz, C. K. Shum, R. S. Nerem, F. J. Lerch, J. A. Marshall, S. M. Klosko, N. K. Pavlis, and R. G. Williamson, 1996. The joint gravity model 3. *Journal of Geophysical Research*, 101, pp. 28029-28049.